The Design Process for Monolithically Manufactured Millimeter-Wave Antenna Arrays Using Stereolithography 3D Printing

Dominik Langer[#1], Bartosz Tegowski[#2], Nils C. Albrecht[#3], Marvin Wenzel[#4], Alexander Koelpin[#4]
[#]Institute of High Frequency Technology, Hamburg University of Technology, Germany
{[1]dominik.langer, [2]bartosz.tegowski, [3]nils.albrecht, [4]marvin.wenzel, [5]alexander.koelpin}@tuhh.de

***Abstract* — This paper presents a design flow enabling monolithic structures for milimeter-wave (mmW) applications utilizing cost-effective stereolithography (SLA). Particular emphasis is given to the design of complex shaped, phase-adjusted 3D waveguide interconnects that allow array elements to be arranged on any three-dimensional or two-dimensional grid. A horn antenna array at 61 GHz with 19 elements fed by a radial power divider is designed, manufactured, and validated. Simulations and measurements show excellent agreement.**

***Keywords* — 3D-printing, additive manufacturing, waveguide, stereolithography (SLA), millimeter wave, antenna array.**

I. Introduction

When millimeter-wave (mmW) frequencies and high demands concerning gain come together, for example, in modern radar systems [1] or satellite communication [2], arranging horn antennas as a waveguide-based array is a suitable solution. However, designing an array of commercially available waveguide components or individual milled parts manufactured as a split block limits the design options for the antenna.

Additive manufacturing techniques are nowadays a viable option for producing high-frequency components to overcome these limitations. Publications show the performance of the various manufacturing processes up to the THz range [3]. Utilizing the stereolithography (SLA) process, components such as [4], [5] have been proposed without monolithically integrating them into a functional array.

Standard software for designing waveguide networks and systems is not intended to take advantage of the degrees of freedom that 3D printing allows. The designs created with standard software use 3D printing only as an alternative manufacturing process.

This paper demonstrates the design process for monolithic mmW antenna arrays using cost-effective SLA. In contrast, the proposed design process allows connecting waveguide ports arranged arbitrarily in three-dimensional space while tuning the phase angle. This way, the array elements can be arranged on any three-dimensional or two-dimensional grid. The advantages of waveguide technology, such as low losses, wide bandwidth, and high-quality factor, can thus be used for antenna arrays regardless of the complexity of the feed network. Milled metal parts or 3D-printed split block assemblies cannot realize feed networks designed according to this paper. Only monolithic 3D-printing has sufficient degrees of freedom for manufacturing. To verify the design process, the authors manufactured and measured A horn antenna array with 19 elements arranged on a hexagonal grid fed by a radial power divider designed for the 61 GHz ISM-Band.

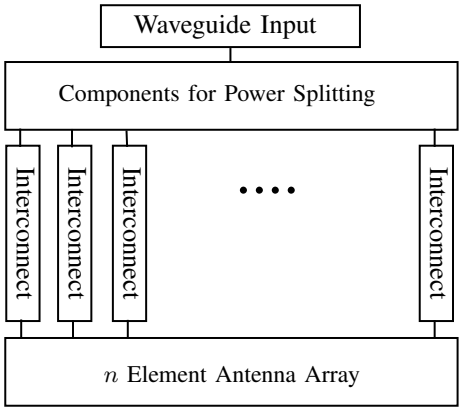

Fig. 1. Representation of an antenna array as a block diagram.

This publication is structured as follows. Section II explains the design process and the antenna array. Section III details the example horn antenna array and Section IV reports the fabrication of the demonstrator and discusses the measured results. In Section V, a conclusion is given.

II. Design Process

Fig. 1 shows the schematic of an antenna array. It consists of components for power splitting, array elements, and the corresponding interconnects. Designing n individual interconnects for n antennas in the array may be necessary. The correct phase angle must feed to the waveguide ports of the power-splitting components and antennas, even if they are offset along the three spatial directions and rotated independently about the longitudinal and transverse axes.

Fig. 2 shows the design process necessary for such arrangements as a flowchart. The different colors symbolize the three different types of software that are required. The blue rectangles indicate work steps in full-wave simulation software. Yellow rectangles depict the steps in a 3D-CAD application for mechanical design. The red rectangles are steps in slicing software, a 3D printer-specific software used to prepare the models for 3D printing.

The components are designed and arranged in the wanted relative geometry before the interconnects are optimized to compensate for different phase delays. The design flow shown in Fig. 2 divides into the upper half, which contains the

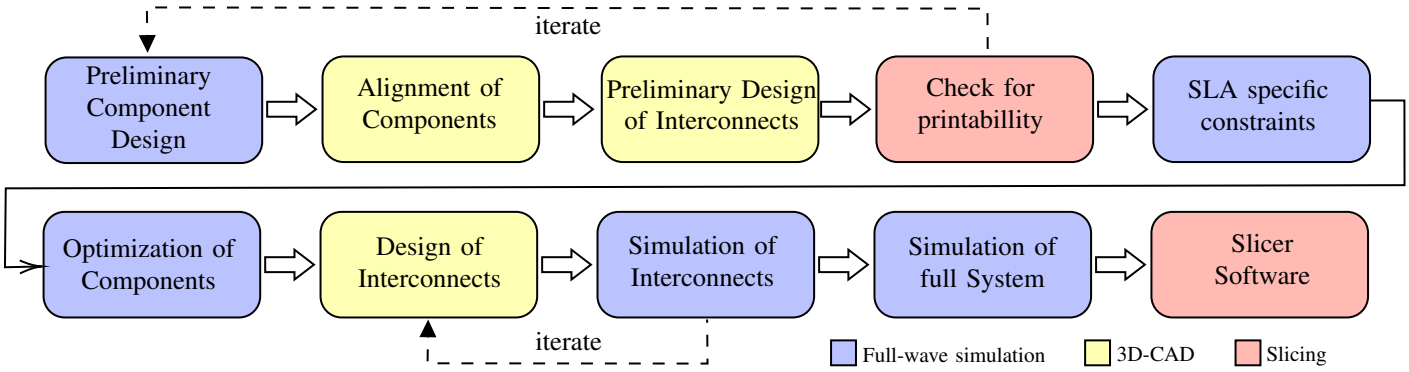

Fig. 2. Visualization of the design process as a flowchart.

preliminary design, and the lower half, which structures the finalization of the design.

A. Preliminary Design

1) Preliminary Component Design

The preliminary design of components for power splitting does not differ from classical manufacturing methods. It is essential to consider the fundamental limitations arising from the resolution of the SLA process. When designing components using SLA, it is crucial to include all necessary features and details in the model while ensuring functionality. Avoid extensive optimization of the components at this stage.

2) Alignment of Components

Now an arrangement in three-dimensional space can be carried out. This method enables the arrangement of components above and next to each other, even if the waveguide ports are not aligned within one plane. In contrast, components manufactured using the split-block technique, as in [6] or [7], must be arranged on a plane.

3) Preliminary Design of Interconnects

Fig. 3(a) shows an example of two RWG cross-sections spaced along the z-axis and x-axis, aligned parallel to the yz-plane. The cross sections are rotated 90° relative to each other, whereby the height of the waveguides differs by a factor of two. The waveguides created by this method compensate for all these differences simultaneously in one continuous sweep. The sweeping function in 3D-CAD software allows the definition of splines along which a cross-section is guided to create a three-dimensional object. Non-uniform rational B-splines (NURBS) [8] form the basis of the splines. The spline's order, the number of control points, and the knot vector define them. In Fig. 3(a), the control points are blue dots, and the knot vector is visualized as a dashed line. The curve order equals the number of control points in the 3D-CAD software since manipulating a single control point always affects the entire curve [8].
For the example in Fig. 3(a), a spline with four control points is used. The individual control points can be adjusted to change the length of the knot vector between them. The length changes the weights of the individual sections, so

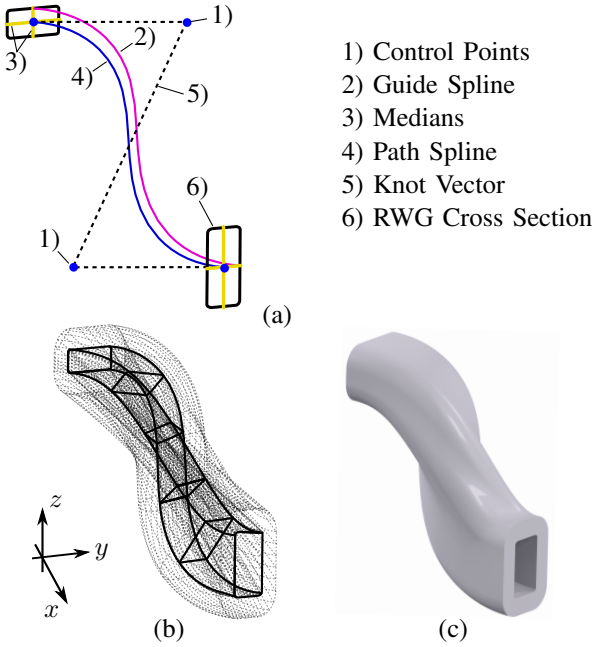

Fig. 3. (a) Illustration of splines connecting two crossections, (b) the resulting cuboid and (c) the final waveguide.

the shape of the curvature and the bending radius can be influenced. The knot vector must be normal to the waveguide cross-sections to ensure a continuous connection of the waveguides. Accordingly, only the length of the knot vector can be varied at the ports. The path spline depicted in blue in Fig. 3(a), connects the waveguide port centers. It defines the bends necessary to overcome the offset along the x- and z-axis. Specifying a guide spline, depicted in purple in Fig. 3(a), defines the cross-section's rotation and scaling along the path spline. The guide spline is connected to the end of the median line of the dimension to be scaled. The median lines in Fig. 3(a) are depicted in yellow. The guide spline must also start as a surface normal, so the same restrictions as for the path spline apply. The spacing and offset between the splines control the waveguide's scaling and rotation along the path spline.
The resulting cuboid connecting the two cross sections is

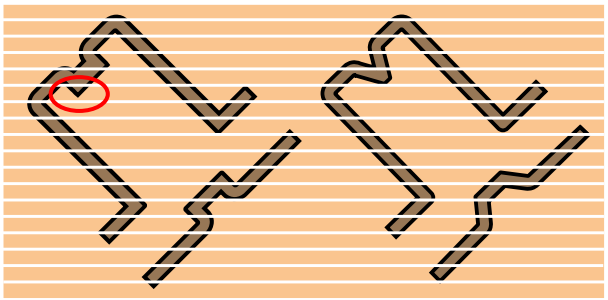

Fig. 4. (a) Visualization of a component that cannot be printed due to internal structures and (b) a version optimized for printing.

depicted as solid lines in Fig. 3(b). The shelling tool creates the final RWG with the desired wall thickness shown as a rendering in Fig. 3(c).
The phase delay along the twisted waveguide interconnects must be adjusted as defined for each interconnect to ensure the desired excitation of the antennas. In that case, the most extended connection should be determined. With the 3D-CAD software's measuring tool, the path spline's length can be determined so that all subsequently designed splines can be adapted. Due to the different curvature, a full-wave simulation is necessary to determine the exact phase rotation.

4) *Check for Printability*

The slicer software creates the necessary support structures and gives a slice-by-slice representation. It also checks if the structure is printable. Due to the monolithic construction, removing internal support structures is impossible. Therefore, checking whether the 3D printer can print the interior features without support structures is essential.
Fig. 4 shows a cut plane through two exemplary waveguide components. The individual layers from which the 3D print is built are colored beige. The support structures are omitted for the sake of simplicity. Two opposing rectangular structures in the center of the component are used in Fig. 4(a). As the print builds up from the lowest to the highest layer, the 3D printer prints the corner marked with the red circle without any connection to the component. Therefore internal support structures would be required. In every printing orientation, the 3D printer will either print a part of the rectangular structures without connection to the component or a large overhang, leading to considerable deformations. Fig. 4(b) shows the truncated triangles which solve this problem. Therefore the component does not need internal support structures because the overhangs are omitted. The corners outside the component are not critical because they are connected to the rest of the three-dimensional component.

5) *Stereolithography (SLA) specific constraints*

When designing waveguide components to be printed using SLA, the limitations of the process must be understood and considered. Limitations regarding resolution for minimum feature size can be found in the 3D printer manufacturer's white papers or must be determined experimentally. Due to the finite resolution, the corners and edges of the simulation models should be rounded off for the most accurate reproduction. An edge radius of 100 µm is used for this work. The rounding of the corner also increases the quality of the metallization.

B. *Final Design*

The lower half of Fig. 2 contains the workflow for the final design. The work steps for the final design are comparable to traditional manufacturing processes. The designed components are optimized and the interconnecting waveguides are iterated between CAD and full-wave simulation. After the full-wave simulation of the whole array, the characteristic can be evaluated.Then the model is exported and transferred to the slicer software for printing.

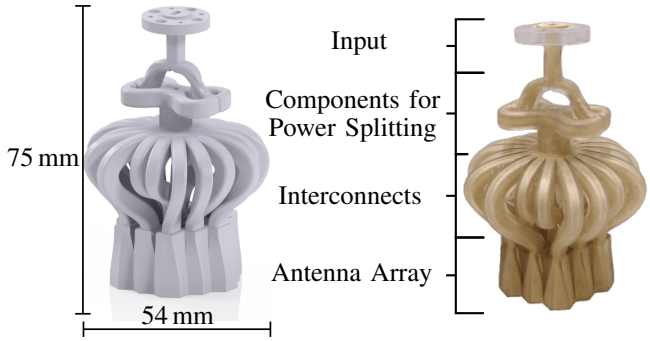

Fig. 5. Comparison between the CAD rendering on the left and a photo of the silver plated 3D-printed antenna array on the right.

III. Antenna Array

The Authors designed an example antenna array to demonstrate the proposed design process. As shown in Fig. 5, it consists of a standard WR-15 waveguide as input and a radial power divider, according to [6], as the power splitting component. Fig. 7(a) shows the 19 hexagonal horn antennas arranged on a hexagonal grid. A single element is a RWG transitioned to a hexagonal aperture. The linearly polarized antennas use the TE_{10}-mode of the RWG.
Fig. 7(b) illustrates the complexity of the interconnects. The dashed line shows the power divider above the antenna inputs. The colored arrows show the different polarization angles of the waveguide ports and mark the ports that must be connected.

IV. Manufacturing and Characterization

The antenna is printed with a *Form3+* from *Formlabs* with clear resin at a layer thickness of 50 µm. The 3D-printed component was cleaned with isopropanol and the surface was cured with an UV lamp. In order to coat only the inner walls of the 3D-printed structure with a conductive layer, an electroless silver plating process was used. It is based on the Tollens' reagent, also known as the Tollens silver mirror test. The reaction solution used is based on [9] and was pumped through the components according to [5].

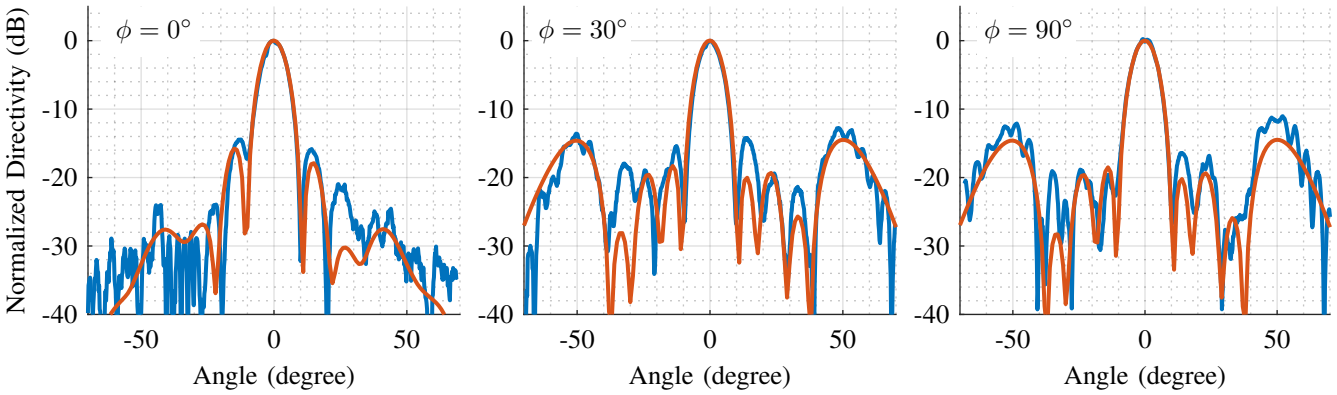

Fig. 6. Comparison between the radiation pattern's (orange) simulation results and (blue) measurement results.

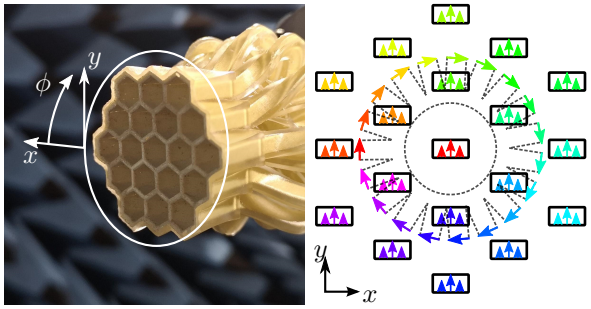

(a) (b)

Fig. 7. (a) Photo of the antenna aperture and (b) a schematic top view of the radial power splitter and the RWG inputs of the horn antennas.

A. Radiation Pattern Measurement

The radiation pattern was measured in an anechoic chamber using a reference antenna and a network analyzer. The antenna's gain is obtained by the direct comparison method. Fig. 6 depicts the normalized directivity in cutting planes at $\phi = 0°$, $\phi = 30°$, and $\phi = 90°$. Besides a slightly higher grating lobe level, the overall agreement between simulation and measurement is excellent. The antenna array with in-phase excitation and uniform power distribution shows a negligible 0.1° wider half-power beam width of 8.8° than in the simulation. The measured gain of the antenna is 21.4 dBi. Due to inhomogeneities in the silver layer, the gain is 4.5 dB lower than in the simulation. It is unknown whether the thickness of the layer, the surface roughness, or the conductivity is the decisive factor. Individual bright spots in the antenna's aperture, visible in Fig. 7(a) , suggest that gas bubbles accumulating on the structure's walls during the metallization process are part of the problem.

V. Conclusion

A novel design process for monolithic mmW antenna arrays is presented, enabling the use of three-dimensional arranged waveguide components interconnected by complex-shaped waveguides.
The design process was validated using an antenna array with 19 hexagonal horn antennas. Its geometrical complexity is beyond the applicability of classical fabrication methods, e.g., milling. The excellent agreement between the simulation and the measurement results of the manufactured antenna validates the proposed design and fabrication process, which provides a solution for fabricating highly complex waveguide components and systems.

Acknowledgment

This work was partly funded by the Deutsche Forschungsgemeinschaft (DFG, German Research Foundation) – SFB 1483 – Project-ID 442419336, EmpkinS.

References

[1] C. Will, K. Shi, S. Schellenberger, T. Steigleder, F. Michler, R. Weigel, C. Ostgathe, and A. Koelpin, "Local pulse wave detection using continuous wave radar systems," *IEEE Journal of Electromagnetics, RF and Microwaves in Medicine and Biology*, vol. 1, no. 2, pp. 81–89, 2017.
[2] J. Zhang, X. Li, Z. Qi, Y. Huang, and H. Zhu, "Dual-band dual-polarization horn antenna array based on orthomode transducers with high isolation for satellite communication," *IEEE Transactions on Antennas and Propagation*, vol. 70, no. 10, pp. 9247–9259, 2022.
[3] A. Hofmann, K. Lomakin, M. Sippel, and G. Gold, "Additively manufactured slotted waveguides for THz applications," in *2022 IEEE/MTT-S International Microwave Symposium - IMS 2022*, 2022, pp. 695–698.
[4] H. Yao, S. Sharma, R. Henderson, S. Ashrafi, and D. MacFarlane, "Ka band 3D printed horn antennas," in *2017 Texas Symposium on Wireless and Microwave Circuits and Systems (WMCS)*, 2017, pp. 1–4.
[5] W. Liu, Z. Chen, T. Viola, and G. H. Huff, "3-d printed directional couplers in circular waveguide," *IEEE Microwave and Wireless Components Letters*, vol. 31, no. 6, pp. 561–564, 2021.
[6] Q.-X. Chu, D.-Y. Mo, and Q.-S. Wu, "An isolated radial power divider via circular waveguide TE_{01}-mode transducer," *IEEE Transactions on Microwave Theory and Techniques*, vol. 63, no. 12, pp. 3988–3996, 2015.
[7] T. Freialdenhoven, P. Witte, and T. Dallmann, "3D printed and metallized ka-band orthomode transducer for polarimetric radar applications," in *2021 15th European Conference on Antennas and Propagation (EuCAP)*, 2021, pp. 1–4.
[8] D. F. Rogers, in *An Introduction to NURBS*, ser. The Morgan Kaufmann Series in Computer Graphics, D. F. Rogers, Ed. San Francisco: Morgan Kaufmann, 2001.
[9] J. Shen, M. Aiken, C. Ladd, M. D. Dickey, and D. S. Ricketts, "A simple electroless plating solution for 3D printed microwave components," in *2016 Asia-Pacific Microwave Conference (APMC)*, 2016, pp. 1–4.